THE JOURNAL OF BIOLOGICAL CHEMISTRY
Vol. 276, No. 42, Issue of October 19, pp. 38844–38851, 2001

Printed in U.S.A.

Hemoglobin-degrading, Aspartic Proteases of Blood-feeding Parasites

SUBSTRATE SPECIFICITY REVEALED BY HOMOLOGY MODELS*

Received for publication, March 2, 2001, and in revised form, August 6, 2001
Published, JBC Papers in Press, August 8, 2001, DOI 10.1074/jbc.M101934200

Ross I. Brinkworth‡, Paul Prociv§, Alex Loukas¶, and Paul J. Brindley‖**

From the ‡Institute of Molecular Biosciences and §Department of Microbiology and Parasitology, University of Queensland, Brisbane, Queensland 4072, Australia, ¶Division of Infectious Diseases and Immunology, Queensland Institute of Medical Research, Brisbane, Queensland 4029, Australia, and ‖Department of Tropical Medicine, School of Public Health and Tropical Medicine, Tulane University, New Orleans, Louisiana 70112

Blood-feeding parasites, including schistosomes, hookworms, and malaria parasites, employ aspartic proteases to make initial or early cleavages in ingested host hemoglobin. To better understand the substrate affinity of these aspartic proteases, sequences were aligned with and/or three-dimensional, molecular models were constructed of the cathepsin D-like aspartic proteases of schistosomes and hookworms and of plasmepsins of *Plasmodium falciparum* and *Plasmodium vivax*, using the structure of human cathepsin D bound to the inhibitor pepstatin as the template. The catalytic subsites S5 through S4′ were determined for the modeled parasite proteases. Subsequently, the crystal structure of mouse renin complexed with the nonapeptidyl inhibitor *t*-butyl-CO-His-Pro-Phe-His-Leu [$CHOHCH_2$]Leu-Tyr-Tyr-Ser-NH_2 (CH-66) was used to build homology models of the hemoglobin-degrading peptidases docked with a series of octapeptide substrates. The modeled octapeptides included representative sites in hemoglobin known to be cleaved by both *Schistosoma japonicum* cathepsin D and human cathepsin D, as well as sites cleaved by one but not the other of these enzymes. The peptidase-octapeptide substrate models revealed that differences in cleavage sites were generally attributable to the influence of a single amino acid change among the P5 to P4′ residues that would either enhance or diminish the enzymatic affinity. The difference in cleavage sites appeared to be more profound than might be expected from sequence differences in the enzymes and hemoglobins. The findings support the notion that selective inhibitors of the hemoglobin-degrading peptidases of blood-feeding parasites at large could be developed as novel anti-parasitic agents.

Blood flukes, hookworms, and the malaria parasites are among the most important pathogens of humans in terms of both numbers of people infected and the consequent morbidity and mortality (1). Although phylogenetically unrelated, these parasites all share the same food source; they are obligate blood feeders, or hematophages. Hb from ingested or parasitized erythrocytes is their major source of exogenous amino acids for growth, development, and reproduction; the Hb, a ~64-kDa tetrameric polypeptide, is comprehensively catabolized by parasite enzymes to free amino acids or small peptides. Intriguingly, all these parasites appear to employ cathepsin D-like aspartic proteases to make initial or early cleavages in the Hb substrate (2–4).

The vertebrate endopeptidase, cathepsin D (EC 3.4.23.5), is a member of the aspartic protease category of hydrolases, which also includes renin, pepsin, chymosin, cathepsin E, HIV[1] protease, and several other enzymes (5, 6). Cathepsin D is expressed in a diverse range of mammalian cells and tissues and is located predominantly in lysosomes (6). The molecule comprises two rather similar lobes, each incorporating a homologous Asp-Thr-Gly catalytic site motif, with the substrate binding groove located between these lobes. In aspartic proteases generally, the nucleophile that attacks the scissile bond of the substrate is an activated water molecule held in position by side chains of the two active-site aspartic acids (5). Well defined S4, S3, S2, S1, S1′, S2′, S3′, and S4′ subsite pockets for the amino acid side chains of the substrate (5) are additional hallmarks of these enzymes. A peptide analogue of microbial origin, pepstatin, is the definitive, general inhibitor of aspartic proteases (7). In general, human cathepsin D is specific for hydrophobic patches in proteins, with an ostensibly anomalous, additional preference for glutamate in the P2 position (8–11).

An improved understanding of the substrate affinity of cathepsin D-like proteases of blood-feeding parasites for Hb could facilitate the development of novel anti-parasite inhibitors. To this end, sequences or models of the cathepsin D-like aspartic proteases of schistosomes and hookworms and of plasmepsins of *Plasmodium falciparum* and *Plasmodium vivax* (PDB file 1QS8) were aligned with and/or three-dimensional, molecular models were constructed, using the structure of human cathepsin D bound to pepstatin (1LYB) (12) as the template. Subsequently, the crystal structure of the peptidic inhibitor CH-66 complexed with mouse renin (1SMR) (13) was used to build homology models of octapeptide substrates. The molecular models were then used to examine the similarities and differences among known substrate cleavage sites in mammalian Hb reported previously for the cathepsin D of *Schistosoma japonicum* (4) and for human cathepsin D (11). The models revealed that the difference in cleavage sites was due, in general, to a

* This work was supported by Australian National Health and Medical Research Council (NHMRC) Grant 971432, the University of Queensland (Australian Research Committee Small Grants Scheme 98/ARCS211G), and the Center for Infectious Diseases, Tulane University. Alex Loukas is an NHMRC Howard Florey Centenary Fellow. Paul Brindley is a recipient of a Burroughs Wellcome Fund Scholar Award in Molecular Parasitology. The costs of publication of this article were defrayed in part by the payment of page charges. This article must therefore be hereby marked "*advertisement*" in accordance with 18 U.S.C. Section 1734 solely to indicate this fact.

** To whom correspondence should be addressed: Dept. of Tropical Medicine, SL29A, Tulane University Health Sciences Center, 1430 Tulane Ave., New Orleans, LA 70112. Tel.: 504-988-4645; Fax: 504-988-6686; E-mail: pbrindl@tulane.edu.

[1] The abbreviation used is: HIV, human immunodeficiency virus.

single amino acid alteration in the cleavage site (P4-P4′) that either enhances or diminishes the enzymatic activity.

EXPERIMENTAL PROCEDURES

Molecular Models of Cathepsin D-like Peptidases—Molecular modeling of the mature forms of the target aspartic proteases was carried out on a Silicon Graphics work station using the Insight II software package from Molecular Simulations Inc. (San Diego, CA), as described previously for several papain-like, cysteine proteases (14–16) and the Swiss Model server. Models were viewed using Swiss PDBViewer. The Insight II module, Homology, was used for the homology modeling. Homology operates by copying the backbone atoms and β-carbons from the template molecule to the model and adding the new side chains. Epitopes corresponding to α-helix or β-sheet in the template are assigned coordinates as structurally conserved regions, whereas other regions are assigned coordinates as designated loops. The Loop Search function was used to find suitable loops, from protein structures in the PDB data base, which have the correct number of residues and distance to bridge and in which the adjacent residues have the appropriate conformations. Molecular models of the cathepsin D-like enzymes of the blood flukes, *S. japonicum* (17) and *Schistosoma mansoni* (18), the hookworm, *Ancylostoma caninum* (19), and plasmepsins I and II of *P. falciparum* (20, 21) were built using the Homology module. The crystal structure of human cathepsin D complexed with the inhibitor pepstatin, PDB number ILYB (12), was used as the template (12). In addition, the crystal structure of *P. vivax* plasmepsin complexed with pepstatin (1QS8) was compared and contrasted with these models. Construction of the homology models was based on previously determined sequence alignments (12, 13, 17–19) but refined according to known secondary structure. In the sequence alignments (shown below under "Results"; see Fig. 1), residues that have side chains participating in substrate binding pockets are indicated as the S5 to S4′ subsites, respectively. In the case of the schistosome and hookworm proteases, the COOH-terminal domain extensions, which are ~40 amino acid residues in length (17–19), were omitted, because they could not be modeled in this way. These proteases have three loops that differ from human cathepsin D, including the latter's cleaved hairpin loop, and the Loop Search function was used to assign possible coordinates for the loops of the *Schistosoma* cathepsin D proteases. The hookworm enzyme has an additional, unusual feature, two small loops, both of which are closed with disulfide bonds, Cys^{92}-Cys^{97} and Cys^{210}-Cys^{217}. Although the function of the loops has not yet been determined, they do not appear to be structurally important for catalysis. A homology model was also built of human cathepsin D, based on itself, with the residues in the hairpin loop deleted and replaced by a single glycine. This was done so that docking with substrate peptides could be carried out similarly with all the other proteases. In each case, the model was minimized to a root mean square deviation of 0.000001, employing conjugate gradients using the Discover module of Insight II. Subsequently, the accuracy and validity of the models was tested with the Profiles 3D module of Insight II, which performs Eisenberg analysis (22).

Homology Models of Peptidase-Octapeptide Substrate Complexes—The crystal structure of mouse renin complexed with the peptidic inhibitor CH-66 (1SMR) (13) was used to build homology models of octapeptide substrates within the catalytic clefts of *S. japonicum* cathepsin D, human cathepsin D, and several other peptidases for which three-dimensional homology models had been constructed. CH-66 is *t*-butyl-CO-His-Pro-Phe-His-Leu[$CHOHCH_2$]Leu-Tyr-Tyr-Ser-NH_2, and the complex of CH-66 within the active site groove of mouse renin is an informative example, with regard to the proteases and substrates targeted in this study, of an extended peptide (P5 to P4′) analogue bound to an archetypal aspartic protease. It was anticipated that this complex would indicate subsite binding pockets in human cathepsin D and homologous aspartic proteases. Loop Search was used to replace the P1 and P1′ isostere residues of the inhibitor with an extended dipeptide and to assign coordinates to the P1 and P1′ residues.

The core and key substrate binding residues of mouse renin and human cathepsin D were superimposed using the α-carbons so that the peptidase and substrate models were in the same space coordinates to conserve the pattern of hydrogen bonding between the enzyme and the backbone peptide bonds of the substrate. For the mouse renin·CH-66 complex, the protease residues forming hydrogen bonds with the main chain of the inhibitor are Gly^{37}, His^{79}, Ser^{80}, Gly^{81}, Asp^{220}, Gly^{222}, Ser^{219}, Ser^{222}, and Thr^{200}, whereas Asp^{35} and Asp^{220} are the catalytic dyad of aspartic acids (numbering according to Fig. 1) (13). Notably, these are consistent with the hydrogen bonding between human renin and the inhibitor CP-85339 (13). The backbone atoms of human cathepsin D and mouse renin are not completely identical; differences in the conformations have been noted for the S3, S2′, and S3′ pockets (12, 13). These differences produce renin subsite pockets that are less open, giving rise to the narrow specificity of this enzyme. Renin also has a higher degree of secondary structure, with some longer stretches of α-helix and β-sheet. Nonetheless, the appropriate pair of enzyme and substrate was associated as an assembly and minimized with only atoms in the side chains remaining unfixed. In some cases, the correct rotamer for the side chain of the substrate residue had to be selected empirically to avoid major clashes with the enzyme. As a result, the substrate models were effectively docked with the peptidase models.

Amino Acid Sequence Alignments—Sequence alignments of the mature regions of the peptidases were prepared using Insight II software from Molecular Simulations Inc. and empirically refined by hand. Subsequently, to accommodate different colors, the alignment presented here was prepared using MacVector 6.5.3 software (Oxford Molecular) and edited manually to replicate the structural alignment generated with Insight II.

Modeled Substrates—Homology models were constructed of aspartic proteases complexed with the peptides KPIEF*FRL, FLSF*PTTK, LVTL*AAHL, and LDKF*LASV (where * represents the characterized or predicted scissile bond). FLSFPTTK, LVTLAAHL, and LDKFLASV are octapeptides found in α-chain of human Hb, as residues 33 to 40, 107 to 114, and 126 to 133, respectively. KPIEFFRL is a synthetic peptide known to be a high affinity substrate for human cathepsin D (23).

RESULTS

Substrate Subsite Binding Pockets—Fig. 1 presents the sequence alignments of the deduced mature enzyme amino acid sequence of *A. caninum* cathepsin D-like protease, human cathepsin D, *S. japonicum* cathepsin D, *S. mansoni* cathepsin D, *P. falciparum* plasmepsin I, plasmepsin II, and mouse renin. The three-dimensional structures of human cathepsin D, plasmepsin II, and mouse renin have been determined previously (12, 13, 24, 25). The sequence alignment was based firstly on structural alignment, with residues found in consensus regions of secondary structure (α-helix, β-sheet) in human cathepsin D, *P. falciparum* plasmepsin II, and mouse renin underlined. The remaining sequences were aligned taking into account the positions of conserved Cys, Gly, and Pro residues, as well as aromatic and hydrophobic residues in structurally conserved regions. The ~30 residues that constitute each subsite of the various cathepsin D-like, Hb-degrading peptidases, including *P. vivax* plasmepsin (1QS8) are listed in Table I, illustrating not only the overall conservation of these residues but also subsite differences among these peptidases. The allocation of residues to the pockets differs somewhat from others reported previously, particularly with respect to the S3′ and S4′ subsites (8, 9, 12, 13), because it was assumed that the conformation of the inhibitor-complexed enzyme mimics that of its substrate-bound form. Profiles 3D analysis (22) of the molecular models indicated a high probability of correct folding, with very few residues defined as being misfolded (not shown).

Cleavage of Hemoglobin—The cleavage of mammalian Hb by human cathepsin D has been reported recently (11), as have the cleavage sites in human Hb for cathepsins D of *S. japonicum* and *S. mansoni* (4). Hydrolysis of Hb by *S. japonicum* cathepsin D involves a generally discrete set of cleavages for the α-chain, compared with cleavage sites for human cathepsin D, whereas these two enzymes share most of the same cleavage points for the β-chain (Fig. 2) (4, 11). The orthologous sequences at these known cathepsin D cleavage sites for bovine, human, and canine Hb are also listed in Fig. 2, although this does not imply that those sites indicated for other substrate species will be cleavage sites for that particular enzyme in every case. This scheme does not reflect the relative importance of each cleavage site or their order. Further, some sites in the Hb α-chain are adjacent, including $Leu^{105} \downarrow Leu^{106}$, $Thr^{108} \downarrow Leu^{109}$, and $Leu^{109} \downarrow Ala^{110}$; cleavage at any one of these would probably obviate cleavage at

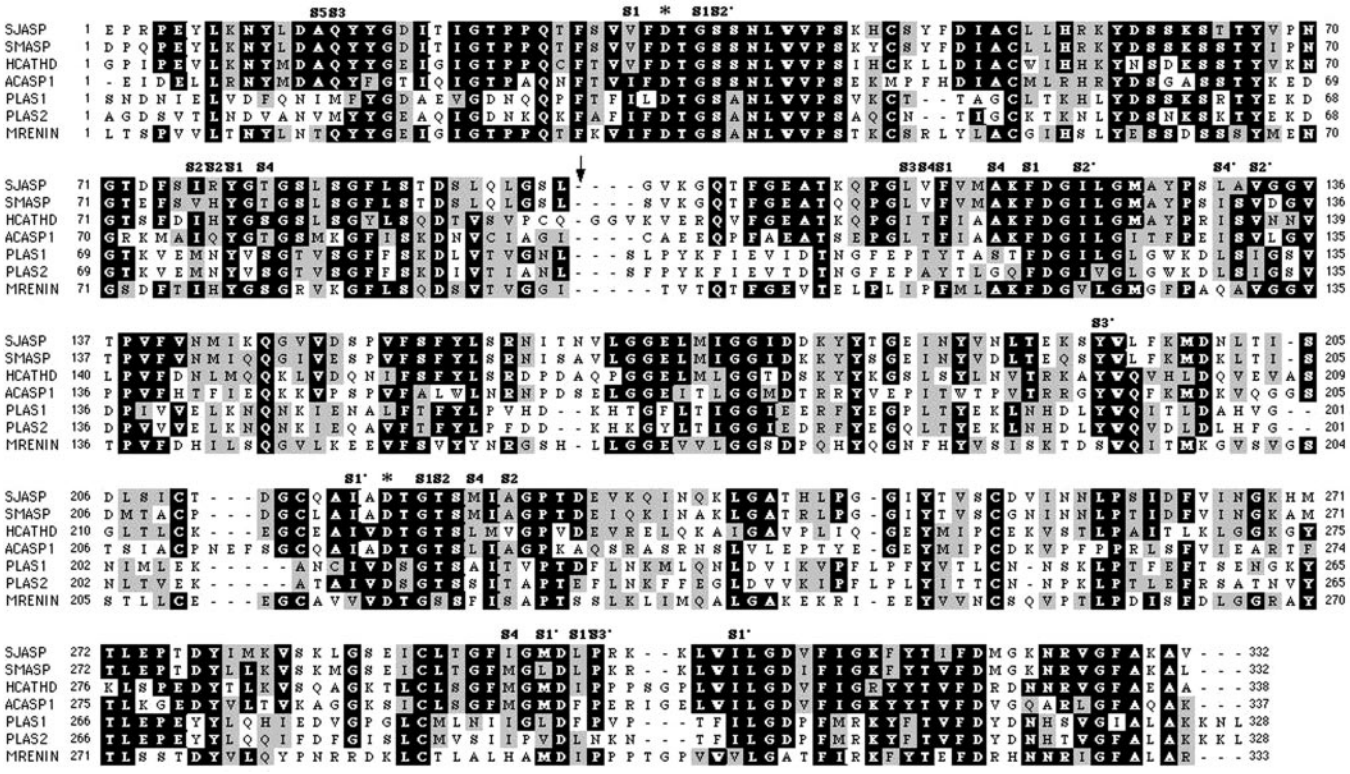

FIG. 1. **Sequence alignment of amino acids of six aspartic proteases based on secondary structure and sequence homology.** The mature enzyme domains only of the proteases enzymes are shown. *SJASP*, the cathepsin D-like protease of the Asian blood fluke *S. japonicum* (L41346); *SMASP*, the cathepsin D-like protease of the African blood fluke *S. mansoni* (U60995); *HCATHD*, human cathepsin D (P07339); *ACASP1*, the cathepsin D-like protease of the hookworm *A. caninum* (U34888); *PLAS1*, plasmepsin I of the malaria parasite *P. falciparum* (X75787); *PLAS2*, plasmepsin II of *P. falciparum* (L10740); and *MRENIN*, renin from the mouse (P06281). Residues that have side chains participating in substrate binding pockets are indicated by their subsite numbers (*S5-S4′*). The dyad of catalytic aspartic acids residues is indicated with *asterisks*. The *arrow* indicates the position of loop 3 in human cathepsin D, the site of processing to a two-chain form (see Refs. 6 and 12). *Black boxes* with *white letters* show identical residues, and *gray boxes* with *black letters* show chemically similar residues.

the vicinal sites. Perhaps the most striking of all these cathepsin D cleavage sites is FLSF↓PTTK (residues 33–40 of the human Hb α-chain), for schistosomal enzyme (4), because a substrate with a proline residue at P1′ appears to be rare or even unique for a eukaryotic aspartic protease.

Molecular Models—Each of the protease and protease·substrate complex models minimized to a plausible structure with no significant defects. However, for reasons of brevity and clarity, much of the analysis and discussion presented here focus on the cathepsin D-like protease from *S. japonicum*. Profiles 3D analysis (19) of the model of this enzyme gave a value of 151, compared with an overall self-compatibility score of 151 and a lowest possible score of 68. This is a high figure, indicating a high probability that the model is correct. The only site of possible misfolding is the loop 46–54, which is well clear of the substrate binding cleft. Fig. 3 shows the general conservation of fold between the apoenzymes of human and *S. japonicum* cathepsins D; side chains of residues that constitute the subsite binding pockets are highlighted. To further investigate the magnitude of sequence variation in the subsite binding pockets and the associated implications for substrate affinities, molecular models of human cathepsin D complexed with KPIEF↓FRL, and of *S. japonicum* cathepsin D with three discrete octapeptides from human Hb, are presented in Fig. 4 (*panels A*, *B*, *C*, and *D*, respectively). Specific details of the modeled complexes are provided below.

Human Cathepsin D Modeled with KPIEFFRL at Its Active Site Cleft—KPIEFFRL is a high affinity substrate for recombinant human cathepsin D (23). Lys at P5 is mostly exposed to the solvent. Ala^{13} makes contact with β-methylene of the P5 Lys. P4 Pro is mostly in hydrophobic contact with Leu^{236}, whereas Ile at P3 is predominantly in hydrophobic contact with Thr^{118} (methyl) and Gln^{14} (β-methylene). For Glu at P2, the carboxyl forms a hydrogen bond with the hydroxyl group of Ser^{80}, and the β-methylene contacts Thr^{227}. However, because Ser^{80} is known to hydrogen bond with the P2 NH of the inhibitor main chain (13), this is not certain. The P1 Phe makes hydrophobic interactions with Phe^{104}, Phe^{119}, and Tyr^{78} of the protease, and Phe at P1′ makes hydrophobic interactions with Ile^{313}, Ile^{222}, and Met^{302}. Arg at P2′ is mostly exposed to the solvent, though there are minor contacts with the β-methylene of His^{77} and with Ile^{135}. Leu at P3′ makes hydrophobic contact with Ile^{222} and Tyr^{198} (Fig. 4, *panel A*). The model explains why KPIEFFRL is a high affinity substrate for human cathepsin D; it makes numerous contacts with the active site of the peptidase.

Modeled Complex of S. japonicum Cathepsin D with LVTLAAHL at Its Active Site Cleft—LVTLAAHL represents residues 107 to 114 of the α-chain of human Hb. It is a cleavage site for both human and schistosome cathepsins D (Fig. 2) (4, 11). Leu at P4 has considerable hydrophobic contact with Met^{224}. Val at P3 has hydrophobic contacts with Val^{114} and Gln^{14}, whereas Thr P2 has hydrophobic contacts with Thr^{222}. Leu at P1 makes hydrophobic contacts with Tyr^{78} and Phe^{115}, and P1′ Ala makes hydrophobic contacts with Ile^{306} and Ile^{217}. The Ala at P2′ makes weak contact with the β-methylene of Ser^{36}. With the P3′ His, the imidazole ring is mostly solvated, and the epsilon methenyl makes contact with Ile^{217} and some contact with Tyr^{194}. Leu at P4′ has some hydrophobic contact with Ile^{131} (Fig. 4, *panel B*). Each of these interactions can also be achieved with human cathepsin D/LVTLAAHL (not shown), which explains why this is a cleavage site for both enzymes.

TABLE I

Residues that constitute the subsite binding pockets, S5 to S4′, of human cathepsin D (HuCathD), cathepsins D from Schistosoma japonicum and S. mansoni (abbreviated here as Sj and Sm CathD, respectively), and Ancylostoma caninum (AcASP-1), plasmepsins I and II of Plasmodium falciparum (Pf), and plasmepsin from P. vivax (Pv), as determined by three-dimensional homology modeling

Residues that differ between the parasite enzymes when compared with human cathepsin D are shown in bold. Catalytic dyad aspartic acid residues are annotated with an asterisk.

Subsite	HuCathD	Sj/Sm CathD	AcASP-1	Pf plasmepsin I/II	Pv plasmepsin
S5	Ala^{13}	Ala^{13}/Ala^{13}	Ala^{11}	**Ile^{14}/Val^{14}**	**Ile^{13}**
S3	Gln^{14}	Gln^{14}/Gln^{14}	Gln^{13}	**Met^{15}/Met^{15}**	**Met^{15}**
S1	Val^{31}	Val^{31}/Val^{31}	**Ile^{30}**	**Ile^{32}/Ile^{32}**	**Ile^{32}**
Catalytic	Asp^{33}*	Asp^{33}*/Asp^{33}*	Asp^{32}*	Asp^{34}*/Asp^{34}*	Asp^{34}*
S1′	Gly^{35}	Gly^{35}/Gly^{35}	Gly^{34}	Gly^{36}/Gly^{36}	Gly^{36}
S2′	Ser^{36}	Ser^{36}/Ser^{36}	Ser^{35}	Ser^{37}/Ser^{37}	Ser^{37}
S2′	Ile^{76}	Ile^{76}/**Val^{76}**	Ile^{75}	**Met^{75}/Met^{75}**	**Ile^{75}**
S2′	His^{77}	**Arg^{77}**/His^{77}	**Gln^{76}**	**Asn^{76}/Asn^{76}**	**Thr^{76}**
S1	Tyr^{78}	Tyr^{78}/Tyr^{78}	Tyr^{77}	Tyr^{77}/Tyr^{77}	Tyr^{77}
S4	Ser^{80}	**Thr^{80}/Thr^{80}**	**Thr^{79}**	Ser^{79}/Ser^{79}	Ser^{79}
S3	Ile^{124}	**Leu^{113}/Leu^{113}**	**Leu^{112}**	**Pro^{113}/Pro^{113}**	**Pro^{113}**
S3/S1	Thr^{125}	**Val^{114}/Val^{114}**	Thr^{113}	Thr^{114}/**Ala^{114}**	Ile^{114}
S1	Phe^{126}	Phe^{115}/Phe^{115}	Phe^{114}	**Tyr^{115}/Tyr^{115}**	**Tyr^{115}**
S4	Ala^{129}	Ala^{118}/Ala^{118}	Ala^{117}	**Ser^{118}/Gly^{118}**	**Val^{118}**
S3/S1	Phe^{131}	Phe^{120}/Phe^{120}	Phe^{119}	Phe^{120}/Phe^{120}	Phe^{120}
S2′	Ile^{134}	Ile^{123}/Ile^{123}	Ile^{122}	Ile^{123}/Ile^{123}	Ile^{123}
S4′	Ile^{142}	**Leu^{131}**/Ile^{131}	Ile^{130}	**Leu^{131}/Leu^{131}**	**Leu^{131}**
S2′	Val^{144}	Val^{133}/Val^{133}	Val^{132}	**Ile^{133}/Ile^{133}**	**Ile^{133}**
S3′	Tyr^{205}	Tyr^{194}/Tyr^{194}	Tyr^{193}	Tyr^{192}/Tyr^{192}	Tyr^{197}
S1′/S3′	Ile^{229}	Ile^{217}/Ile^{217}	Ile^{220}	Ile^{212}/Ile^{212}	Ile^{212}
Catalytic	Asp^{231}*	Asp^{219}*/Asp^{219}*	Asp^{222}*	Asp^{214}*/Asp^{214}*	Asp^{214}*
S1	Gly^{233}	Gly^{221}/Gly^{221}	Gly^{224}	Gly^{216}/Gly^{216}	Gly^{216}
S2	Thr^{234}	Thr^{222}/Thr^{222}	Thr^{225}	Thr^{217}/Thr^{217}	Thr^{217}
S4	Leu^{236}	**Met^{224}/Met^{224}**	Leu^{227}	**Ala^{219}/Ser^{219}**	**Thr^{218}**
S2	Val^{238}	**Ala^{226}/Ala^{226}**	**Ala^{229}**	**Thr^{221}/Thr^{221}**	**Thr^{221}**
S4	Met^{307}	**Ile^{295}**/Met^{295}	Met^{298}	**Ile^{290}/Ile^{290}**	**Leu^{290}**
S1′/S2	Met^{309}	Met^{297}/**Leu^{297}**	Met^{300}	**Leu^{292}/Val^{292}**	**Val^{292}**
S1′/S3′	Ile^{311}	**Leu^{299}/Leu^{299}**	**Phe^{302}**	**Phe^{294}/Leu^{294}**	Ile^{294}
S3′	Pro^{312}	Pro^{300}/Pro^{300}	Pro^{303}	Pro^{295}/**Asn^{295}**	Asp^{295}
S1′	Ile^{320}	Ile^{308}/Ile^{308}	Ile^{311}	Ile^{300}/Ile^{300}	Ile^{300}

Model of S. japonicum Cathepsin D with LDKFLASV at Its Active Site Cleft—LDKFLASV represents residues 126 to 133 of the α-chain of human Hb. *S. japonicum* cathepsin D cleaves at this site, whereas the human enzyme does not (Fig. 2) (4, 11). In the model (Fig. 4, *panel C*), Leu at P4 makes extensive hydrophobic contacts with Met^{224}, Asp at P3 hydrogen bonds to Gln^{14}, and Lys at P2 makes hydrophobic contacts with Thr^{222}. Further, the epsilon amino group of the P2 Lys hydrogen bonds to main chain at residues Leu^{225} and Ala^{226}. The latter is not possible with human cathepsin D (not shown), perhaps explaining why this site is not cleaved by human cathepsin D. The Phe at P1 makes hydrophobic interactions with Tyr^{78}, Phe^{115}, and Phe^{120} of the schistosome peptidase. Leu at P1′ has extensive hydrophobic interactions with Ile^{306}. The Ala at P2′ has weak contact with the β-methylene of Ser^{36} and Arg^{77}. Arg^{77} has a different conformation from that in *panel B*. The Ser at P3′ has a minor contact with Tyr^{194}, whereas the P4′ Val has considerable hydrophobic contact with Leu^{131}.

Model of S. japonicum Cathepsin D with FLSFPTTK at Its Active Site Cleft—FLSFPTTK represents residues 33 to 40 of the α-chain of human Hb. As with LDKFLASV (above), it is a cleavage site for schistosome but not human cathepsin D (Fig. 2). Again, this is an unusual cleavage site, in that a PI′ Pro represents an ostensibly rare substrate preference for a eukaryotic aspartic peptidase. As shown in Fig. 4, *panel D*, Phe at P4 has hydrophobic contacts with Met^{224} and Ile^{295}, and Leu at P3 has hydrophobic contacts with Val^{114}. The P2 Ser hydrogen bonds to Thr^{222} through the hydroxyls. The Phe at P1 contacts methyl groups of Val^{114} and Thr^{80} (these contacts are not possible with the human enzyme). The P1 Phe also contacts Tyr^{78} and Phe^{120}, but not the Phe^{116}, of the S1 pocket. Backbone atom locations in P2, P1, and P1′ differ considerably from those in modeled complexes of *S. japonicum* cathepsin D with LVTLAAHL or LDKFLASV, described above. The Pro P1′ has weak hydrophobic contacts with Ile^{306} and possibly Thr^{222} but does not contact the Ile^{217} at S1′/S3′. The Thr P2′ makes weak contacts with Ser^{36} but is mostly solvent-exposed. The Thr at P3′ contacts Ile^{217} and Tyr^{194} but would not contact Ile^{217} if the P1′ residue were larger. The Lys at P4′ is mostly solvent-exposed but has some hydrophobic contact with Leu^{131} (Fig. 4, *panel D*). An additional feature is noteworthy, if enigmatic; the conformation of Arg^{77} of the S2′ pocket (Table I) differs in each of the three *S. japonicum* cathepsin D models presented here (Fig. 4, *panels B*, *C*, and *D*), yet none of the P2′ residues apparently makes meaningful contact with Arg^{77}.

Plasmepsins—Plasmepsins I and II are located in the digestive vacuole of intraerythrocytic stages of the malaria parasite, *P. falciparum*, where they function in the proteolysis of human Hb (20, 21). The crystal structures of plasmepsin II (24) and proplasmepsin II (25) have been reported, and the crystal structure of a plasmepsin of *P. vivax* is available (1QS8). The plasmepsins are too dissimilar to human cathepsin D to be designated cathepsin D-like enzymes, as can be seen in Fig. 1. However, all of the parasite and mammalian enzymes examined here, including the plasmepsins, belong to the same family, family A1 of the pepsin clan (clan AA), according to the phylogeny and nomenclature of Barrett *et al.* (5). This structure-based sequence alignment (Fig. 1) showed 33% identity of

Human cathepsin D - Known cleavage sites in bovine hemoglobin are shown (Ref. 11), alongside orthologous sites in human and canine hemoglobin.

Hemoglobin α-chain

Cleaved	Bovine	Human	Canine
1	V*LSPA	V*LSPA	V*LSPA
24	AAEY*GAEA	AGEY*GAEA	AGDY*GGEA
32	LERM*FLSF	LERM*FLSF	LDRT*FQSF
109	LLVT*LASH	LLVT*LAAH	LLVT*LACH
134	ANVS*TVLT	ASVS*TVLT	AAVS*TVLT
137	STVL*TSKY	STVL*TSKY	STVL*TSKY

Hemoglobin β-chain

Cleaved	Bovine	Human	Canine
6	TAEE*KAAV	TPEE*KSAS	TAEE*KSLV
14	VTAF*WGKD	VTAL*WEKV	VSGL*WGKV
30	LGRL*LVVY	LGRL*LLVV	LGRL*LIVY
31	GRLL*VVYP	GRLL*VVYP	GRLL*IVYP
40	TQRF*FESF	TQRF*FESF	TQRF*FDSF
44	FESF*GDLS	FESF*GDLS	FDSF*GDLS
53	ADAV*MNNF	PDAV*MGNP	PDAV*MSNA

***Schistosoma japonicum* cathepsin D** – Known cleavage sites in human hemoglobin are shown (Ref. 4), alongside equivalent sites in bovine and canine hemoglobin.

Hemoglobin α-chain

Cleaved	Bovine	Human	Canine
29	AEAL*ERMF	AEAL*ERMF	GEAL*DRTF
33	ERMF*LSFP	ERMF*LSFP	DRTF*QSFP
36	FLSF*PTTK	FLSF*PTTK	FQSF*PTTK
45	YFPH*FDLS	YFPH*FDLS	YFPH*FDLS
109	LLVT*LASH	LLVT*LAAH	LLVT*LACH
110	LVTL*ASHL	LVTL*AAHL	LVTL*ACHH
129	LDKF*LANV	LDKF*LASV	LDKF*FAAV

Hemoglobin β-chain

Cleaved	Bovine	Human	Canine
6	TAEE*KAAV	TPEE*KASV	TAEE*KSLV
14	VTAF*WGKD	VTAL*WEKV	VSGL*WGKV
30	LGRL*LVVY	LGRL*LLVV	LGRL*LIVY
31	GRLL*VVYP	GRLL*VVYP	GRLL*IVYP
40	TQRF*FESF	TQRF*FESF	TQRF*FDSF
44	FESF*GDLS	FESF*GDLS	FDSF*GDLS
129	LQAD*FQKV	VQAA*YQKV	VQAA*YQKV

FIG. 2. **Known and predicted cleavage sites for *S. japonicum* and human cathepsins D in mammalian (human, bovine, and canine) hemoglobin.** Peptide bond cleaved after residue indicated. Residues marked with *underlines* show the presence of substitutions in orthologous amino acids. The hemoglobin sequences were obtained from the public domain; the data base accession numbers for the bovine hemoglobin α- and β- chains are P01966 and P022070, for the canine hemoglobin α- and β-chains they are P01952 and P02056, and for the human hemoglobin α- and β-chains they are NP000508 and NP000509. Some of the information for this figure was obtained from Refs. 4 and 11.

plasmepsin II with human cathepsin D and 31% for plasmepsin I. Blastp analysis revealed that the mature form of the *P. vivax* plasmepsin (1QS8) is 31% identical to human cathepsin D and 70% identical to plasmepsin II of *P. falciparum*. In all three plasmepsins examined here, about half of the substrate binding residues of human cathepsin D are conserved (Table I). Plasmepsin I of *P. falciparum* cleaves the human Hb α-chain at residue 33 (ERMF ↓ LSFP), residue 46 (FPHF ↓ DLSH), and residue 98 (VNFK ↓ LLSH) and the β-chain at residues 31 (LGRL ↓ LVVY), 41 (TQRF ↓ FESF), and 129 (VQAA ↓ YQKV) (2). *P. falciparum* plasmepsin II cleaves the human Hb α-chain at residues 33 (ERMF ↓ LSFP), 108 (LLVT ↓ LAAH), and 136 (STVL ↓ TSKY) and the β-chain at residue 32 (GRLL ↓ VVYP) (2). These differences in cleavage sites may be the reason for having (at least) two plasmepsins; the combination of cleavages by both plasmepsins may deliver Hb fragments small enough for further processing by other peptidases. The oligopeptide Ala-Leu-Glu-Arg-Thr-Phe ↓ Phe-Ser-Phe-Pro-Thr has been proposed as an ideal plasmepsin II substrate, based on the ERMF ↓ LSFP cleavage site (24).

As shown in Table I, the S4, S3, S2, S1, and S2′ subsites of the malarial plasmepsins differ considerably from those of the human, schistosome, and hookworm cathepsins D, possibly explaining the fewer Hb cleavage sites for the *P. falciparum* plasmepsins. The presence of Ala^{219} (instead of Leu or Met, present in the human, schistosome, and hookworm cathepsins D) ensures a more open S4 pocket, which would accommodate the binding by large hydrophobic residues such as Phe. It would also allow binding by hydrophilic and charged residues, such as Glu, although this is not evident from the known Hb cleavage sites (2). However, the *P. falciparum* plasmepsins I and II and the *P. vivax* plasmepsin all retain a Ser equivalent to Ser^{80} of human cathepsin D (Table I), which suggests that they would have a similar P2 specificity for Glu residues. Another similarity with the human enzyme is the presence of an equivalent residue to Thr^{125} in the S3/S1 pockets (Thr^{114} in plasmepsin I) (Table I), which would prevent plasmepsin I from cleaving FLSFPTTK (not shown), a site cleaved by the schistosome cathepsins D (see Fig. 2 and Fig. 4*D*) but not by the human cathepsin D or *P. falciparum* plasmepsins I and II (2, 11).

DISCUSSION

Hemoglobin-degrading enzymes of hematophagous parasites are being targeted for the rational development of novel antiparasitic compounds (26, 27). Given that Hb is the natural substrate of these enzymes, comparison of their cleavage sites in the molecule with the cleavage site profile of homologous mammalian-host enzymes, such as human cathepsin D, is likely to provide specific leads that could be exploited in inhibitor design. However, information on the Hb-cleavage patterns for human schistosomes has not been available until recently. Accordingly, by focusing here on the specific substrate cleavage patterns known for schistosome cathepsin D (4) and human cathepsin D (11), we undertook a molecular modeling analysis of some representative shared and discrete cleavage sites. This involved the docking of octapeptides representing the P4-P4′ residues of Hb cleavage sites that were either common to both schistosome and human cathepsins D or cleaved by one but not the other.

Using the crystal structures of human cathepsin D complexed with pepstatin and mouse renin complexed with CH-66 as guides for the models, ~30 residues could be identified as major contributors to substrate or inhibitor binding in the panel of target parasite and mammalian aspartic proteases (Table I). Eight of these catalytic subsite residues differed between human and *S. japonicum* cathepsins D. Such an ostensibly minor difference between these two enzymes raised the question as to why they do not cleave the α- and β-chains of Hb at exactly the same sites; of the 13 cleavage sites reported for both the mammalian (11) and *S. japonicum* cathepsin D (4), only six are shared (Fig. 2). As depicted in Fig. 4, homology models of the *S. japonicum* and/or human enzyme complexed with four informative octapeptides allowed examination of their subsite binding pockets. Whereas other, usually hydrophilic, residues can occur in any of the peptide subsites, their side chains do not interact with the enzyme. Glycine residues can also be found. Further, the exact nature of the Hb cleavage sites would depend on the order of cleavage, because an adjacent site may obscure its neighbor.

The S4 subsite is essentially a hydrophobic pocket. In human cathepsin D, it comprises Leu^{236} and Met^{307}. These are replaced with Met or Ile in the *S. japonicum* and *S. mansoni* cathepsins D, changes that would have minimal influence on the specificity of this pocket. Residues preferred by human cathepsin D at P4 include Leu, Val, Thr, Pro, and Ala (8–11). The S3 pocket comprises Gln^{14}, Ile^{124}, Thr^{125}, Ala^{129}, and Phe^{131}, and Met, Ile, Ser, and Thr are preferred P3 residues. S3 is both a hydrophilic and a hydrophobic pocket, with hydrophilic residues binding to the Gln^{14} side chain and hydrophobic residues binding to the remainder. Longer hydrophobic side chains can reach into the pocket as far as Ala^{129} and possibly

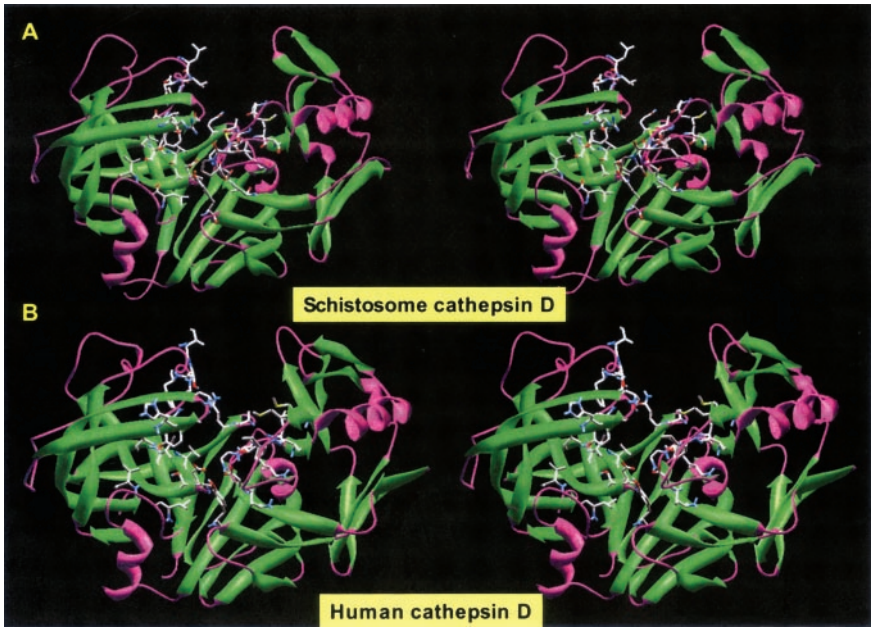

FIG. 3. **Stereo view of molecular model of *S. japonicum* cathepsin D (*panel A*) based on the crystal structure of human cathepsin D (1LYA) (*panel B*).** β-Sheets are shown as *green ribbons*, whereas loops and α-helices are shown as *magenta carbon traces*. Side chains of residues that constitute the subsite binding pockets are *highlighted*. The model was generated using the Swiss Model server and viewed in Swiss PDBViewer.

Phe[131]. Ile[124] is probably too distant to be normally involved in binding, although it could be exploited in inhibitor design. Changing Thr[125] to a Val has little effect on the S3 pocket, because it is the methyl moiety of Thr[125], rather than the hydroxyl, that faces this pocket.

The S2 subsite of human cathepsin D comprises Ser[80], Thr[234], Val[238], and Met[309] (Table I) and exhibits a preference for Glu, Ile, Val, Ala, or Phe at P2 (8–11). Shorter residues, such as Val and Ala, bind to Thr[234], with longer residues such as Met, Ile, or Phe also binding to Val[238] and possibly Met[309]. The major exception is a P2 Glu, which hydrogen bonds to Ser[80], in what is known in aspartic proteases as one of the "flaps" that close over the active site when a peptide is bound (28). As has been demonstrated with the equivalent mouse renin·CH-66 complex (13), the hydroxyl group of Ser[80] normally hydrogen bonds with the P2 amino group of the inhibitor. A putative hydrogen bond with the P2 Glu side chain would have to be a novel feature, unless the Ser hydroxyl can share two hydrogen bonds. This provides the likely reason why human cathepsin D cleaves AAEY ↓ GAEA (residues 21–28, α-chain of Hb) whereas *S. japonicum* cathepsin D does not (Fig. 2), particularly as the P1′ Gly does not contribute to substrate binding. Replacing Ser[80] with Thr, as occurs in the schistosome enzyme (Table I), weakens this hydrogen bond, because the hydroxyl of the Thr adopts a rotamer slightly different from that in Ser. This modifies the P1 pocket, because the methyl group of the Thr now intrudes. Alanine (Ala[226]) instead of Val[238] (Table I) would open up the distal end of the S2 subsite, but this would affect only longer hydrophilic residues, such as lysine, at the P2 position. These models of *S. japonicum* cathepsin D indicate that the epsilon-amino group of a P2 Lys (*e.g.* see Fig. 4*C*) would be able to hydrogen bond to the carbonyl oxygen of the Ile residue immediately preceding the Ala. This option would be blocked with human cathepsin D, providing the likely explanation why *S. japonicum* cathepsin D, but not the human enzyme, cleaves LDKF ↓ LASV (residues 126–133, Hb α-chain). Note that a P2 Arg is possible for human cathepsin D, as can be seen with several of the mammalian Hb cleavage sites (Fig. 2), because the guanidino group of Arg can be considerably solvated (more so than Lys), thereby stabilizing the enzyme·substrate complex. The larger S2 site in the *Schistosoma* enzyme probably accounts for its cleavage of ERMF ↓ LSFP (Hb α-chain, residues 30–37) with Met at the P2 position. Human cathepsin D cleaves the adjacent LERM ↓ FLSF site. The sole Hb α-chain cleavage site common to both human and *S. japonicum* cathepsins D is LLVT ↓ LAAH (α-chain residues 106–113) (Fig. 2). This contains residues that both proteases can readily accommodate, including valine at P2. However, the adjacent LVTL ↓ AAHL is a cleavage site only for *S. japonicum* cathepsin D.

The S1 subsite in human cathepsin D comprises Val[31], Asp[33], Tyr[78], Thr[125], Phe[126], Ile[229], Asp[231], and Gly[233] and exhibits a preference for Leu, Tyr, Phe, or Ile as P1 residues. Clearly, this is a very hydrophobic subsite that can accommodate the side chains of Leu and Phe. The two changes, Ser[80] to Thr and Thr[125] to Val, observed with both *Schistosoma* cathepsins D, render that side of the S1 pocket even more hydrophobic than that of human cathepsin D. This becomes important with the schistosomal cathepsin D cleavage of FLSF ↓ PTTK. The P1′ proline residue readily fits into the S1′ subsite. However, the change in the peptide backbone affects the location and conformation of the Phe at P1. With the *S. japonicum* cathepsin D, Phe at P1 can bind to the methyl groups of Thr[80] and Val[114]. With human cathepsin D, by contrast, the hydrophilic hydroxyl of Thr[125] impedes the binding of a P1 Phe when proline is at P1′. These findings indicate that the octapeptide FLSFPTTK could be a useful lead for developing a specific inhibitor of schistosomal cathepsin D. Development of inhibitors of HIV protease followed the discovery of a similar preference by HIV, type I retropepsin for Pro at P1′ (29, 30).

The S1′ subsite of human cathepsin D comprises Gly[35], Asp[231], Met[309], Ile[311], and Ile[320], and its preferences include Leu, Val, Ala, and Phe at P1′ (8–11). Phe side chains at P1′ adopt one of two conformations. The Phe rotamer found with human and *Schistosoma* cathepsins D faces toward the S2 pocket, with the S-methyl of Met[309] (which arises in the S2 subsite) contacting the β-methylene of the Phe. With the hookworm cathepsin D, which has a S1′ Phe instead of Ile[311], the P1′ Phe adopts a different rotamer, it faces the S3′ subsite, because it is sterically hindered from facing toward Met[309]. This conformation is also adopted for a P1′ Leu for any of the enzymes, because a P1′ Leu cannot reach as far as Met[309]. Consequently, the side chain of the P1′ Phe makes more contacts with the enzyme.

The S2′ subsite of human cathepsin D comprises Ser[36], Ile[76], His[77], Ile[134], Ile[142], and Val[144] and exhibits a preference for

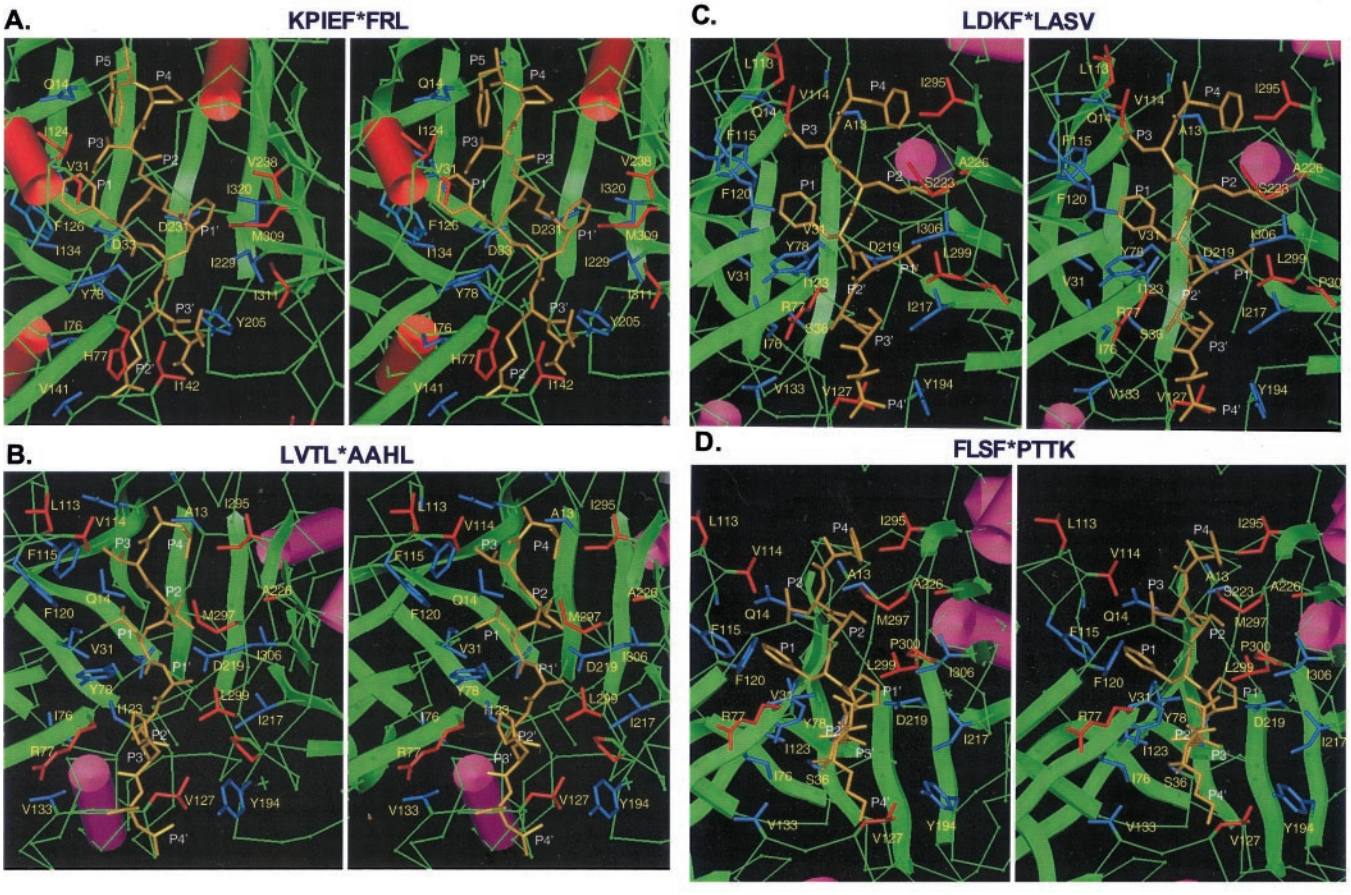

FIG. 4. **Stereo views of the catalytic active sites of molecular models of minimized peptidase·substrate complexes.** β-Sheets are shown as *green ribbons*, and loops and α-helices are shown as *magenta barrels* except for human cathepsin D where helices are shown in *red*. Octapeptide substrates are shown in *mustard* (*yellowish-brownish*), with component residues labeled according to their respective sites of cleavage (*P5-P4′*). The residues corresponding to each substrate peptide are listed *above* the respective *panels*, with *asterisks* denoting the position of the scissile bond. Key subsite residues and their side chains involved in the catalysis are displayed and labeled. *Panel A*, human cathepsin D with octapeptide substrate, KPIEF*FRL; residues shared with *S. japonicum* cathepsin D are shown in *blue* whereas unique residues are *orange*. *Panels B–D*, *S. japonicum* cathepsin D with LVTL*AAHL (*B*), *S. japonicum* cathepsin D with LDKF*LASV (*C*), and *S. japonicum* cathepsin D with FLSF*PTTK (*D*). *S. japonicum* cathepsin D residues shared with human cathepsin D are shown in *blue* whereas unique residues are *red*. The models were constructed using the Molecular Simulations Inc. Insight II modeling package.

Lys, Arg, Glu, or His at P2′. As with the S3 subsite, this pocket should accommodate hydrophobic and hydrophilic side chains, although P2′ hydrophobics are not common (8–11). These models suggest that the functional ends of long basic P2′ residues (Lys and Arg) are mostly exposed to the solvent but that shorter hydrophilic side chains, such as those of Glu and Asp, would be able to hydrogen bond with Ser^{36} or possibly with His^{77}. Replacement of His^{77} with either Arg or Gln will change the order of preferred residues at P2′ but not the overall mix. An Arg at this position may promote the possibility of a P2′ Glu by forming a salt bridge, whereas Gln at this position may promote the possibility of a Gln at P2′ through mutual hydrogen bonding. Hydrophobic residues such as valine can bind to Val^{144}.

The S3′ subsite residues of human cathepsin D are Tyr^{205}, Ile^{311}, and Pro^{312}, and preferences at P3′ include Leu, Lys, Val, Tyr, and Thr (8–11). This is another predominantly hydrophobic pocket. Ile^{311} is variable, affecting both the S1′ and the S3′ pockets, but this would have little influence on subsite specificity. The S4′ pocket is composed of Ile^{142} in human cathepsin D, and its P4′ preferences include Ala, Ser, Val, Lys, Phe, and Tyr. Most of these P4′ amino acids would be exposed to the solvent, but smaller hydrophobic residues such as Ala or Val can bind to Ile^{142}. Mutating the Ile^{142} to Leu in *S. japonicum* cathepsin D (Ile^{131}; see Table I) should have minimal effect on subsite specificity.

It is clear that the differences in Hb cleavage by the proteases examined here reflect subtle yet significant differences in their substrate binding pockets. Development of selective inhibitors of these parasite aspartic proteases as novel anti-infective agents will depend on defining these differences and deriving compounds that exploit one or (preferably) several of them. From an evolutionary perspective, it is straightforward to conceptualize how mutations in Hb genes would lead to amino acid substitutions in their products and how the cumulative effect of such substitutions could then reduce the efficiency of the cognate hemoglobinases of the hematophagous parasite, delivering a selective advantage to the host by reducing the viability or virulence of the parasite. Moreover, as speculated previously (31), the compatibility between an Hb-degrading enzyme of the parasite and the Hb of its mammalian hosts (Fig. 2) is likely to be a critical factor in determining its host range, *i.e.* host specificity. In this regard, it is notable that plasmepsin II has a lower affinity for fetal than for adult Hb, which contributes to the innate resistance of human neonates to malaria (32).

REFERENCES

1. Despommier, D. D., Gwadz, R. W., Hotez, P. J., and Knirsch, C. A. (2000) in *Parasitic Diseases*, 4th Ed., Apple Trees Productions, LLC, New York
2. Gluzman, I. Y., Francis, S. E., Oksman, A., Smith, C. E., Duffin, K. L., and Goldberg, D. E. (1994) *J. Clin. Invest.* **93,** 1602–1608
3. Ghoneim, H., and Klinkert, M.-Q. (1995) *Int. J. Parasitol.* **25,** 1515–1519
4. Brindley, P. J., Kalinna, B. H., Wong, J. Y. M., Bogitsh, B. J., King, L. T,

Smyth, D. L., Verity, C. K., Abbenante, G., Brinkworth, R. I., Fairlie, D. P., Smythe, M. L., Milburn, P. J., Bielefelt-Ohmann, H., Zheng, Y., and McManus, D. P. (2001) *Mol. Biochem. Parasitol.* **112,** 103–112
5. Barrett, A. J., Rawlings, D., Woessner, J. F. (1998) in *Handbook of Proteolytic Enzymes* (Barrett, A. J., Rawlings, D., and Woessner, J. F., eds) pp. 801–805, Academic Press, Oxford
6. Connor, G. E. (1998) in *Handbook of Proteolytic Enzymes* (Barrett, A. J., Rawlings, D., and Woessner, J. F., eds) pp. 828–836, Academic Press, Oxford
7. Rich, D. H., Bernatowicz, M. S., Agarwal, N. S., Kawai, M., Salituro, F. G., and Schmidt, P. G. (1985) *Biochemistry* **24,** 3165–3173
8. van Noort, J. M., and Alfons, C. M. (1989) *J. Biol. Chem.* **264,** 14159–14164
9. Scarborough, P. E., Gurprasad, K., Topham, C., Richo, G. R., Conner, G. E., and Blundell, T. L. (1993) *Protein Sci.* **2,** 264–276
10. Hewitt, E. W., Treumann, A., Morrice, N., Tatnell, P. J., Kay, J., and Watts, C. (1997) *J. Immunol.* **159,** 4693–4699
11. Fruitier, I., Garreau, I., and Piot, J.-M. (1998) *Biochem. Biophys. Res. Commun.* **246,** 719–724
12. Baldwin, E. T., Bhat, T. N., Gulnik, S., Hosur, M. V., Sowder, R. C., Cachau, H. R. F., Collins, J., Silva, A. M., and Erickson, J. W. (1993) *Proc. Natl. Acad. Sci. U. S. A.* **90,** 6796–6800
13. Dhanaraj, V., Dealwis, C. G., Frazao, C., Badasso, M., Sibanda, B. L., Tickle, I. J., Cooper, J. B., Driessen, H. P. C., Newman, M., Aguilar, C., Wood, S. P., Blundell, T. L., Hobart, P. M., Geoghegan, K. F., Ammirati, M. J., Danley, D. E., O'Connor, B. A., and Hoover, D. J. (1992) *Nature* **357,** 466–472
14. Brinkworth, R. I., Brindley, P. J., and Harrop, S. A. (1996) *Biochim. Biophys. Acta* **1298,** 4–8
15. Brinkworth, R. I., Tort, J. F., Brindley, P. J., and Dalton, J. P. (2000) *Int. J. Biochem. Cell Biol.* **32,** 373–384
16. Brady, C. P., Brinkworth, R. I., Dalton, J. D., Dowd, A. J., Verity, C. K., and Brindley, P. J. (2000) *Arch. Biochem. Biophys.* **380,** 46–55
17. Becker, M. M., Harrop, S. A., Dalton, J. P., Kalinna, B. H., McManus, D. P., and Brindley, P. J. (1995) *J. Biol. Chem.* **270,** 24496–24501; Correction, (1997) *J. Biol. Chem.* **272,** 17246
18. Wong, J. Y. M., Harrop, S. A., Day, S. R., and Brindley, P. J. (1997) *Biochim. Biophys. Acta* **1338,** 156–160
19. Harrop, S. A., Prociv, P., and Brindley, P. J. (1996) *Biochem. Biophys. Res. Commun.* **227,** 294–302
20. Goldberg, D. E. (1998) in *Handbook of Proteolytic Enzymes* (Barrett, A. J., Rawlings, D., and Woessner, J. F., eds), pp. 858–860, Academic Press, Oxford
21. Goldberg, D. E. (1998) Plasmepsin II, In *Handbook of Proteolytic Enzymes* (Barrett, A. J., Rawlings, D., and Woessner, J. F., eds), pp. 860–862, Academic Press, Oxford
22. Luthy, R., Bowie, J. U., and Eisenberg, D. (1992) *Nature* **356,** 83–85
23. Beyer, B. M., and Dunn, B. M. (1996) *J. Biol. Chem.* **271,** 15590–15596
24. Silva, A. M., Lee, A. Y., Gulnik, S. V., Maier, P., Collins, J., Bhat, T. N., Collins, P. J., Cachau, R. E., Luker, K. E., Gluzman, I. Y., Goldberg, D. E., and Erickson, J. W. (1996) *Proc. Nat. Acad. Sci. U. S. A.* **93,** 10034–10039
25. Bernstein, N. K., Cherney, M. M., Loestcher, H., Ridley, R. G., and James, M. R. (1999) *Nat. Struct. Biol.* **6,** 32–37
26. Moon, R. P., Bur, D., Loetscher, H., D'Arcy, A., Tyas, L., Oefner, C., Grueninger-Leitch, F., Mona, D., Rupp, K., Dorn, A., Matile, H., Certa, U. Berry, C., Kay, J., and Ridley, R. G. (1998) *Adv. Exp. Med. Biol.* **436,** 397–406
27. McKerrow, J. H. (1999) *Int. J. Parasitol.* **29,** 833–837
28. Tang, J. (1998) in *Handbook of Proteolytic Enzymes* (Barrett, A. J., Rawlings, D., and Woessner, J. F., eds), pp. 806–814, Academic Press, Oxford
29. Dunn, B. M. (1998) in *Handbook of Proteolytic Enzymes* (Barrett, A. J., Rawlings, D., and Woessner, J. F., eds), pp. 919–928, Academic Press, Oxford
30. Copeland, T. D., Wondrak, E. M., Tozser, J., Roberts, M. M., and Oroszlan, S. (1990) *Biochem. Biophys. Res. Commun.* **169,** 310–314
31. Brinkworth, R. I., Harrop, S. A., Prociv, P., and Brindley, P. J. (2000) *Int. J. Parasitol.* **30,** 785–790
32. Shear, H. L., Grinberg, L., Gilman, J., Fabry, M. E., Stamatoyannopoulos, G., Goldberg, D. E., and Nagel, R. L. (1999) *Blood* **92,** 2520–2526

Hemoglobin-degrading, Aspartic Proteases of Blood-feeding Parasites: SUBSTRATE SPECIFICITY REVEALED BY HOMOLOGY MODELS

Ross I. Brinkworth, Paul Prociv, Alex Loukas and Paul J. Brindley

J. Biol. Chem. 2001, 276:38844-38851.
doi: 10.1074/jbc.M101934200 originally published online August 8, 2001
